IJNRD.ORG ISSN : 2456-4184
INTERNATIONAL JOURNAL OF NOVEL RESEARCH AND DEVELOPMENT (IJNRD) | IJNRD.ORG
An International Open Access, Peer-reviewed, Refereed Journal

Effects of Radiations on Satellites Exposed to Extreme Space Weather Events

Dr. Sujatha R,

Associate Professor in Physics

Government first grade College, HSR Layout Bangalore-560102

Abstract

High-energy trapped electrons in the Van Allen belts pose a threat to the survivability of orbiting spacecraft. Two key radiation effects are total ionizing dose and displacement damage dose in components and materials, both of which cause cumulative and largely irreversible damage. During an extreme space weather event, trapped electron fluxes in the Van Allen belts can increase by several orders of magnitude in intensity, leading to an enhanced risk of satellite failure. We use extreme environments generated by modeling and statistical analyses to estimate the consequences for satellites in terms of the radiation effects described above. A worst-case event could lead to significant losses in power generating capability—up to almost 8%—and cause up to four years' worth of ionizing dose degradation, leading to component damage and a life-shortening effect on satellites. The consequences of such losses are hugely significant given our increasing reliance on satellites for a vast array of services, including communication, navigation, defense, and critical infrastructure.

Key Points

- Extreme space radiation environments are used to calculate cumulative engineering effects on spacecraft in geostationary and medium Earth orbits
- Extreme enhancements to trapped electrons in the Van Allen belts cause more cumulative damage than extreme solar energetic particle events
- A temporary enhancement in trapped electron intensity could result in up to 7.6% degradation of solar cell power capacity

Plain Language Summary

Satellites are exposed to a variety of sources of potentially damaging space radiation. One of the most important of these is the population of high-energy electrons that lies trapped by the Earth's magnetic field—the so-called Van Allen belts. During an extreme space weather event, trapped electron fluxes in the Van Allen belts can increase by several orders of magnitude in intensity, leading to an enhanced risk of satellite damage. One example of this damage is degradation in the power-generating capability of satellite solar panels. The threat from space weather in this context has hitherto been associated with solar proton events, that is, bursts of energetic protons that are sporadically emitted from the Sun. However, our analysis shows that enhancements in the Van Allen belt electron population can exceed the solar proton threat, which has implications for the protection of satellites from such phenomena. It is essential that sufficiently robust engineering design measures are put in place, in order to ensure the future reliability of satellite technology, on which our society is increasingly reliant.

1 Introduction

The threat to satellites from high-energy radiation in the space environment is well known (Heynderickx et al., 2004; Horne et al., 2013; Lohmeyer et al., 2015; Maurer et al., 2017). Historically, this existential threat from extreme space weather has often been framed in the context of solar "superstorms" that involve very large fluences of energetic protons produced by shocks associated with coronal mass ejections (CMEs; see Odenwald et al., 2006, or Odenwald & Green, 2007, for example). However, the mechanisms that are responsible for much of the vulnerability are not exclusive to protons. Cumulative effects such as total ionizing dose (TID) and displacement damage are also caused by the populations of trapped energetic electrons that form the Van Allen belts. For example, the injection of energetic electrons could cause additional radiation exposure to satellites undergoing electric orbit raising equivalent to 6.5-year operation at geostationary orbit (Horne & Pitchford, 2015). Here we examine that these effects in the context of orbits most often used for navigation and communication satellites (medium Earth orbit [MEO] and geostationary orbit, respectively), in order to gauge the threat level from trapped electrons in comparison with solar protons. In doing so we test the null hypothesis that in the context of extreme space weather events, solar protons are the dominant cause of degradation, particularly for solar cells.

The focus of this work is on the MEOs used for Global Navigation Satellite Systems (GNSS; inclination 50°–65° and altitude range 18,000–25,000 km) and geostationary Earth orbits (GEOs) where the trapped electron environment in the outer belt is particularly intense and known to cause problems for satellites (Ryden et al., 2008). Short-term enhancements to the electron environment may be caused by CMEs or fast solar wind streams from coronal holes. We do not attempt to distinguish between these two types of enhancement mechanism as each can lead to the same deleterious effects. Protons and heavy ions from galactic cosmic rays (GCRs) and solar energetic particle events (SEPEs) can also cause radiation damage, in terms of both cumulative effects such as TID and displacement damage dose (DDD), and also single-event effects (SEE; Petersen, 1997). SEPEs are stochastic events that cannot be accurately forecast and are not necessarily coincident with extreme electron enhancements in the Van Allen belts (Xapsos et al., 1996). In this paper we contrast the cumulative damage from extreme electron enhancements with that from extreme SEPEs, while noting that a complete analysis of which particle population poses the greater overall threat would need to include a bespoke assessment of the vulnerability of spacecraft components to SEE and indeed the phenomenon of internal dielectric charging (which we will examine in a separate paper). For example, electric orbit raising missions may use trajectories that spend a considerable amount of time in the trapped proton belt, likely resulting in protons being the dominant particle species for displacement damage to solar cells (Messenger et al., 2014).

The EU FP7 SPACESTORM project (**www.spacestorm.eu**) has examined various aspects of the environment and effects during electron enhancements in the Van Allen belt. One part of this work was to use statistical analysis of electron flux and charging current data sets to characterize worst-case events over long time periods in geostationary and MEOs (Meredith et al., 2015, 2016). In addition, the British Antarctic Survey (BAS) radiation belt model (Glauert et al., 2014) has been used to produce a reconstructed 30-year data set of the trapped electron environment in the specific MEO of the Galileo GNSS, from which further deductions of extreme environments can be made. We use these outputs and those from other environment models to quantify the degrading effects on satellites in extreme radiation environments. In this analysis we focus on the following cumulative radiation damage mechanisms:

1. TID: ionization in insulating regions leads to charge trapping and device performance degradation.
2. DDD: atoms in a lattice structure are displaced by incident radiation, leading to *dark* currents, loss of gain in bipolar transistors, and damage to solar cells.

The tools used to calculate the radiation effects described here are available via the online Space Environment Information System (SPENVIS; www.spenvis.oma.be).

2 Environments

For each of our two key orbits we derive worst-case environments from statistical and modeling studies and from applicable trapped radiation models. These may be summarized as follows:

2.1 MEO

BAS have reconstructed a 30-year data set for the Galileo GNSS orbital environment using their comprehensive radiation belt model (BAS-RBM) with GOES >2-MeV electron data as a boundary condition (Glauert, 2016). This data set captures the fluctuations that Galileo satellites would have seen over a 30-year period, which is substantially longer than the operational period of any individual satellite but nonetheless highly relevant to the survivability of the constellation for the long term. The Galileo orbit altitude is approximately 23,222 km, with an inclination of 56°. Equivalent data sets for other orbits of interest can also be reconstructed from the BAS model, enabling a versatile approach to extreme environment analysis. Two representative flux time series from the BAS 30-year reconstructed data set for Galileo are shown in Figure 1. Daily-averaged differential fluxes at 1 and 2 MeV are shown for the whole simulated time period. The so-called *electron desert* in 2009/2010, where the population of trapped electrons in the outer belt dropped significantly, is clearly visible.

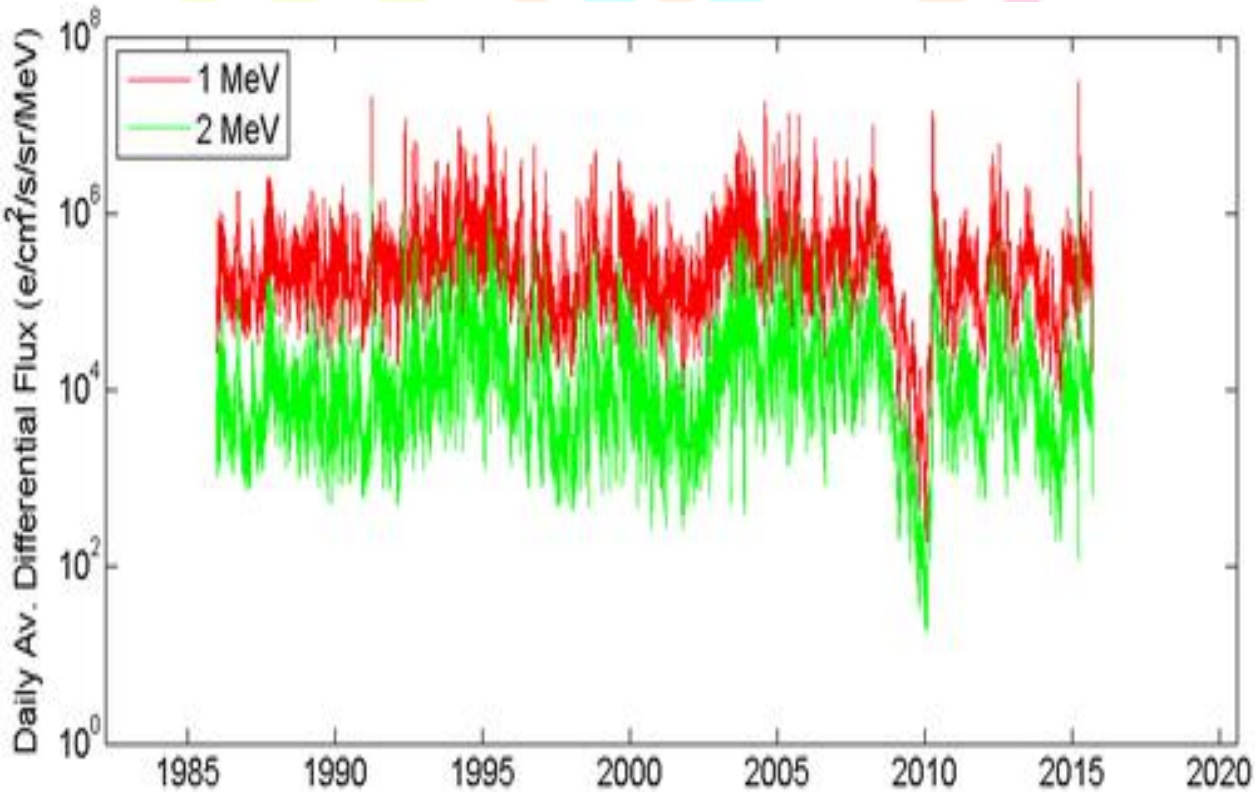

Figure 1
Reconstructed 30-year differential electron flux from the British Antarctic Survey-radiation belt model. The daily average fluxes at 1 and 2 MeV are shown, with the 2009/2010 *electron desert* clearly visible.

From these differential fluxes we are able to construct worst-case electron spectra over different averaging periods (all of which are longer than the orbital period of ~14 hr) by extracting the peak flux in 20 discrete energy bins in the

range 0.5–8 MeV and creating composite spectra from these maxima. These are shown in Figure 2 for the range 0.5–6 MeV. The averaging periods are crucial because the duration of an enhanced environment is an important determinant of the severity of the effect it may have on a satellite. Even an extreme peak in relativistic electron intensity is unlikely to be of significance in engineering terms unless it is sustained for a reasonable length of time, likely to be of the order of at least hours if not days or longer (note that this statement does not apply to low-energy plasma electrons, for which very short timescale enhancements can indeed be a concern). Plotted on the same axes are the predictions of the Model of Outer Belt Electrons for Dielectric Internal Charging (MOBE-DIC) at three exceedance probabilities averaged over a Galileo orbit. MOBE-DIC is an empirical model derived from seven years of electron currents measured on board the Galileo precursor satellite GIOVE-A (Hands et al., 2015), which produces daily average flux spectra as function of magnetic (B, L) coordinates and three exceedance probabilities—90, 99, and 100%. Although MOBE-DIC is primarily aimed at internal charging phenomena, its outputs apply to any effects from temporary electron enhancements in the outer belt. Figure 2 shows that the 95% spectrum from the AE9 static model (Johnston et al., 2014) lies in between the 90 and 99% MOBE-DIC spectra, although the former represents a confidence level and the latter exceedance probabilities, so the comparison is informative rather than validation. As can be seen in Figure 2, the 100% case of MOBE-DIC is very close to the worst-day in the BAS reconstructed data set for the energy range 2–4 MeV. At higher and lower energies the spectra diverge and the BAS worst-day is considerably greater than the MOBE-DIC 100% level. Due to the synodic solar rotation period, the duration of individual enhancements to the intensity of trapped electrons (what might be referred to as *events*) is not likely to greatly exceed one week. This applies to enhancements to the solar wind stream due to coronal holes and to enhancements caused by CMEs from active regions on the solar surface. Hence, we use the worst-week spectrum as the canonical worst-case for our analysis of cumulative radiation effects at MEO.

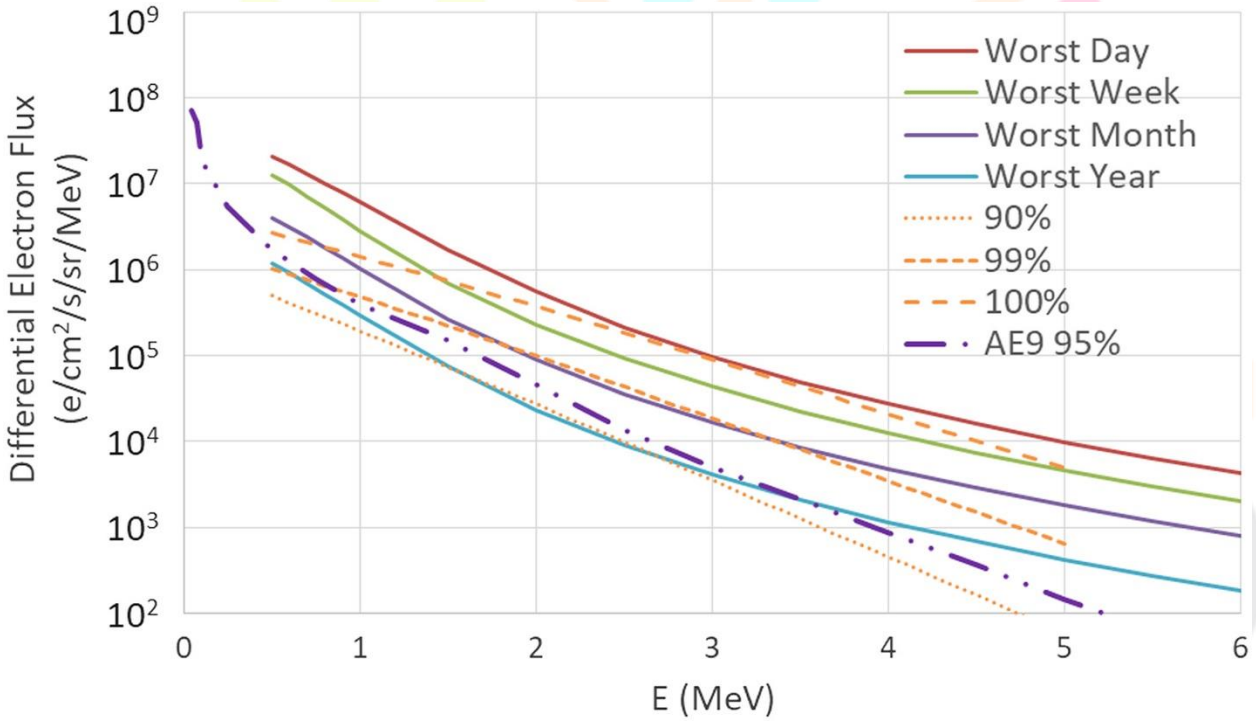

Figure 2

Worst-case spectra from British Antarctic Survey reconstructed 30-year data set, along a Galileo-like medium Earth orbit (solid lines). The *worst-week* spectrum is used for cumulative effects of total ionizing dose and displacement damage dose. Orbit-averaged Model of Outer Belt Electrons for Dielectric Internal Charging fluxes are also shown at three exceedance probabilities (dotted/dashed lines), as is the 95% confidence level spectrum from the AE9 static model.

2.2 GEO

Meredith et al. (2015) conducted an extreme value analysis of $E > 2$ MeV electrons observed by the GOES satellites. Figure 3 shows a comparison of worst-case fluxes in given time periods for two spacecraft in geostationary orbit, relative to a model of the static background. For example, a 1 in 150-year event has an enhancement factor of over

400 relative to the static AE8 model (Vette, 1991) in geostationary orbit. These comparisons are based on one-day average fluxes from GOES satellite data (Meredith et al., 2015). Thus, the appropriate assumption for duration for these events is one day, though it is not unreasonable to assume that the events last longer than this at a similar, if slightly lower, flux (this is addressed quantitatively later on).

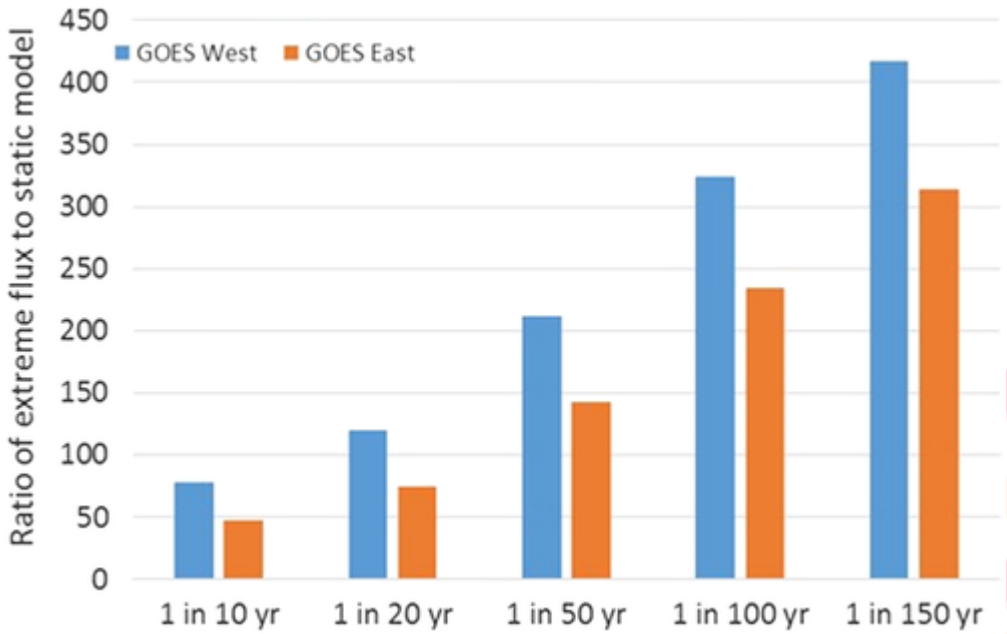

Figure 3

The ratios of extreme electron enhancements at geostationary Earth orbit to the quiescent background in the AE8 model are shown for two GOES satellite locations as a function of recurrence period. The baseline AE8 > 2 MeV integral fluxes at GOES West and East positions are electrons 2.4×10^3 and 1.4×10^3 electrons $\cdot$ cm$^{-2} \cdot$ s$^{-1} \cdot$ sr^{-1}, respectively.

For our radiation effect calculations we use the statistically derived >2 MeV GOES West electron fluxes to renormalize AE8 spectra calculated at GOES West location in GEO. These are shown for the 1 in 10-, 1 in 50-, and 1 in 150-year cases, using the same scale factors for both integral and differential spectra, in Figure 4. Also plotted is the worst-case daily flux at GEO according to the Flux Model for Internal Charging (FLUMIC) model (Rodgers et al., 2003; Wrenn et al., 2000), which is based primarily on GOES data from the 1980s and 1990s. Like MOBE-DIC, FLUMIC is a worst-case model specifying daily average fluxes, primarily aimed at internal charging concerns. However, it is a relevant reference point for worst-case flux estimates aimed at other effects as well. FLUMIC approximates the electron spectrum with a simple exponential function for integral flux, for which the only two free parameters are the normalization and folding energy (E_0). The folding energy varies with date due to inbuilt modulations based on seasonal fluctuations and the solar cycle. We simply adopt the worst case, which gives an exponential folding energy of 0.5. Agreement between FLUMIC and MOBE-DIC is good at GEO (Hands et al., 2015); however, we use FLUMIC for comparison here as it is more widely adopted as a standard for this environment (ECSS-E-ST-10-04C, 2008). For completeness we also plot the 95% worst-case spectrum from the more recent AE9 model (Johnston et al., 2014).

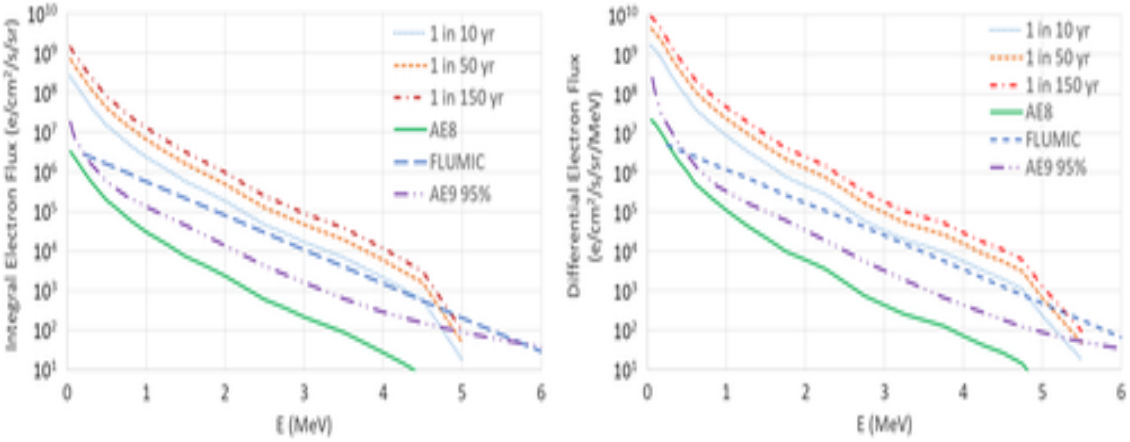

Figure 4

AE8 integral (LHS) and differential (RHS) flux spectra scaled to extreme events in the geostationary environment at three recurrence periods—10, 50, and 150 years. Spectrum from the worst-case Flux Model for Internal Charging (FLUMIC) model and the 95% worst-case from AE9 are also shown for comparison.

It is somewhat unexpected that the FLUMIC fluxes are, in general, below those of the 1 in 10-year event from statistical analysis of GOES data. This probably reflects several differences, including the dead-time correction applied to GOES fluxes by Meredith et al. (2015), and the influence of recent large events on estimated magnitudes at a given recurrence frequency (for example, a major enhancement on 29 July 2004 was deemed to be a 1 in 50-year event). It is worth noting also that the GOES West location, although more severe than GOES East, is not necessarily the worst-case longitude for geostationary orbit radiation intensity (Rodgers et al., 2003).

These spectra at MEO and GEO set the context for our analysis of electron-induced effects. Although the timescales vary somewhat for the derivation of the different *worst-case* environments, this range of specifications will help us understand to what degree the estimation of effects depends on the assumed worst-case environment.

2.3 Proton Environment

The trapped proton environment can pose a major threat to spacecraft in low Earth orbits. At MEO (as defined above by GNSS-relevant orbits) and GEO, however, there is no significant trapped flux at energies that cause radiation damage. The proton and heavy ion threat to spacecraft comes instead from GCRs and SEPEs. The former of these is an approximately steady state background environment of very energetic particles that do not contribute as much as trapped particles to the cumulative damage effects of TID and displacement damage (Taylor et al., 2007). Rather, the threat from GCR is SEE to discrete components such as memories and transistors (Maurer et al., 2017), which are out of our scope of cumulative damage effects.

For space missions, taking SEPEs into account may involve a probabilistic determination of cumulative proton fluence at a specific confidence level for the whole mission lifetime (Xapsos et al., 2000). For this analysis, where worst-case electron effects are based on extreme enhancements during storms, we focus instead on a worst-case individual event. What constitutes a worst-case SEPE depends in part on context (Shea & Smart, 1994; Shea et al., 2006). As for electrons, direct measurements of SEPEs in space instrumentation are limited to the space era. Unlike electrons, however, the most energetic and intense SEPEs can be measured indirectly on the surface of the Earth. For example, the largest event on record with energies sufficient to affect terrestrial systems occurred on 23 February 1956 (Meyer et al., 1956). During this event (known as a ground level enhancement or GLE) a 50-fold increase in count rates at the neutron monitor station in Leeds, UK, was observed. This can be considered as the most extreme (directly measured) space weather event yet observed in the context of radiation threats to terrestrial systems, including

avionics (Tylka & Dietrich, 2009). Even longer timescales may be analyzed using appropriate proxy data. Several methods for inferring the historical occurrence of large SEPE or GLE events have been suggested in the scientific literature (Mekhaldi et al., 2015; Miyake et al., 2012). These involve using proxy data to infer the enhancement of primary (proton) or secondary (neutron) particles in the upper atmosphere. For example, Antarctic ice cores have been used to reconstruct a long-term record of GCR intensity using the relative abundance of beryllium-10, which is created through spallation interactions between cosmic rays and molecules in the upper atmosphere and precipitates down to the ground and is subsequently encapsulated in ice layers. Spikes in ^{10}Be concentration in these long-term (hundreds or even thousands of years) records are then interpreted as enhancements in the radiation environment, from which proton fluences can be calculated. Enhancements in the carbon-14 abundance in ancient trees serve as a similar proxy of primary proton fluence, in this case via the capture of atmospheric thermal neutrons by molecular nitrogen. For space applications, common practice has been to use spectra based on a series of large events observed in October 1989. The CREME96 software package uses these data to provide *worst-day* and *worst-week* proton fluence spectra for SEE calculations (https://creme.isde.vanderbilt.edu/). These timescales relate directly to those we have used for electron enhancements. Analogous to the statistical approach employed by Meredith et al. (2015) to derive extreme electron fluxes, Xapsos et al. used a statistical approach to define a worst-case proton event in their emission of solar proton (ESP) model (Xapsos et al., 1999).

Several of these candidates for worst-case SEPE proton spectra are shown in Figure 5. The different energy ranges of the spectra reflect the different environments that they were established for. For example, the Feb-56 spectrum, as it predates the space era, is based solely on terrestrial measurements that are well suited to quantifying the high energy end of the spectrum. By contrast, the ESP model worst-case spectrum is based on space data and thus is truncated at 500 MeV (as detectors that can reliably measure protons at higher energies than this are rare on spacecraft). For satellites, the key threat is from protons in the tens to hundreds of MeV range, as this covers a substantial fraction of the total SEPE fluence with sufficient energy to penetrate outer spacecraft shielding. The >500 MeV part of the spectrum is primarily of relevance to terrestrial systems, as protons below this threshold are attenuated by the atmosphere without significant production of secondary particles. A large SEPE may typically last for several days, though peak flux periods are more likely to last only for several hours. As the spectrum is provided in terms of fluence rather than flux, the time profile and duration of the event are not important in our calculations. As a further justification, the >30 MeV fluence for the ESP worst-case event is 1.3×10^{10} protons/cm^2, which is similar to that inferred for events occurring once or twice every thousand years from the long-term C-14 record (Usoskin & Kovaltsov, 2012). This is also reflected in recent work done under the auspices of the International Electro-technical Commission (IEC), which defines an extreme space weather event over such timescales as part of its 62396 standards series for avionics (IEC-TS 62396-6, 2017). The analysis, based on cosmogenic isotope records, estimates a 1 in 1,000-year event proton fluence at approximately 30 times greater than the Feb-56 event. We use this enhancement factor applied to the Feb-56 spectrum as an additional category of worst-case SEPE. As can be seen in Figure 5, this puts such an event significantly larger than the ESP worst-case event for >100-MeV protons, but much closer to equivalence for >10-MeV protons. The consequences of this difference in spectral shape are explored in later sections of the paper.

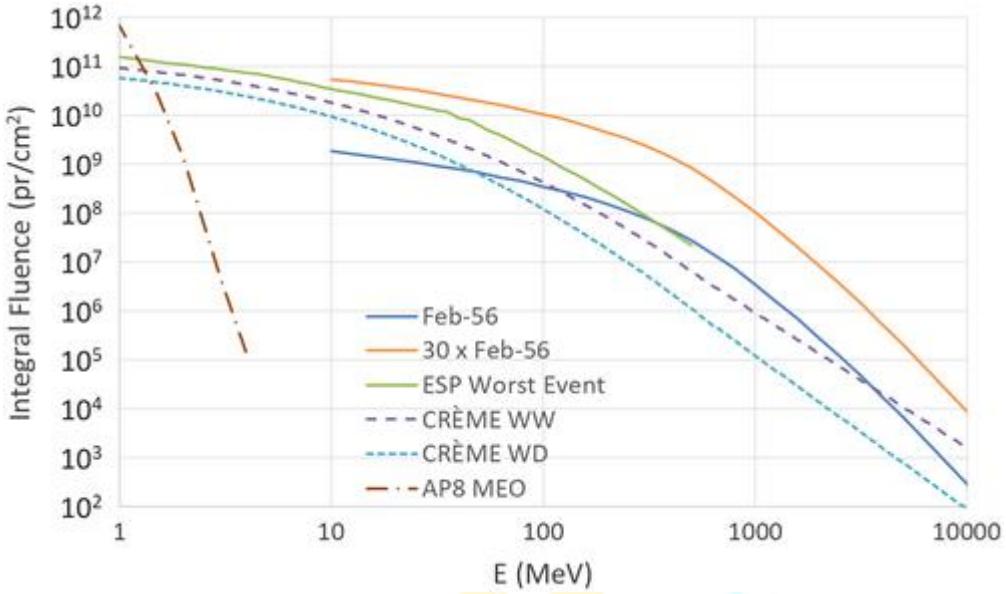

Figure 5
Candidate worst-case SEPE integral proton spectra for effects calculations. The emission of solar proton (ESP) model uses statistical analysis to define a worst-case spectrum. CRÈME worst-week and worst-day spectra are based on October 1989 storms. The Feb-56 event spectrum is based on ground-level measurements. The trapped proton environment averaged over a Galileo-type medium Earth orbit, which is comprised of low-energy protons only, is shown for comparison.

3 TID

TID is a long-term cumulative problem. Ionization in insulating (oxide) layers of semiconductor components leads to the buildup of trapped positive charge, often concentrated at interface boundaries (Oldham & Mclean, 2003). This charge can affect the behavior of the components in a variety of ways, for example, threshold shifts in field effect transistors and off-state leakage currents. If dose levels become too high, then such parametric shifts can cause a component to become totally defective, leading to the loss of critical spacecraft systems. TID is caused by both protons and electrons, with the trapped proton environment particularly significant in low Earth orbit due to the South Atlantic Anomaly (SAA; Ginet et al., 2007). Measurements in MEO (Ryden et al., 2008) during the SEPE of December 2006 showed clearly that protons made a negligible contribution to TID, whereas a subsequent moderate electron enhancement had a much more significant effect. However, the question we address is whether or not this holds for extreme events as well.

In this section we use the SHIELDOSE-II tool (available at www.spenvis.oma.be) to calculate TID in enhanced electron and proton environments as a function of shielding depth, based on spherical geometry. Although the responses of components to TID are extremely variable, the dose calculations below are independent of component, and thus the severity of the various environments can be compared directly. Figure 6 shows a comparison of dose-depth curves for four solar proton scenarios and one extreme electron enhancement scenario at MEO and GEO respectively. No attenuation from geomagnetic shielding is included for the solar proton events as this would not apply to high inclination portions of MEO and would only affect very low energy protons (and hence thin shielding) at GEO. ESP worst event, Feb-56 and 30 × Feb-56 are assumed to be individual proton events, whereas CREME96 WW (worst-week) is a sum over several events from the same active region. The MEO scenario is the worst-week from the BAS model 30-year data set (Figure 2), and the GEO scenario is also predicated on the 1 in 150-year event lasting for one week, with an adjustment factor based on the average ratio between the worst-day and worst-week flux in the MEO data set (this reduces the fluence by approximately a factor of two; i.e., the worst-week fluence is equivalent to 3.5 days' worth of the worst-week flux). For context, commercial off-the-shelf components are often assumed to experience problems when dose exceeds 5 $krad_{[Si]}$, whereas specially manufactured *rad-hard* components should have tolerances in the range 50–300 $krad_{[Si]}$.

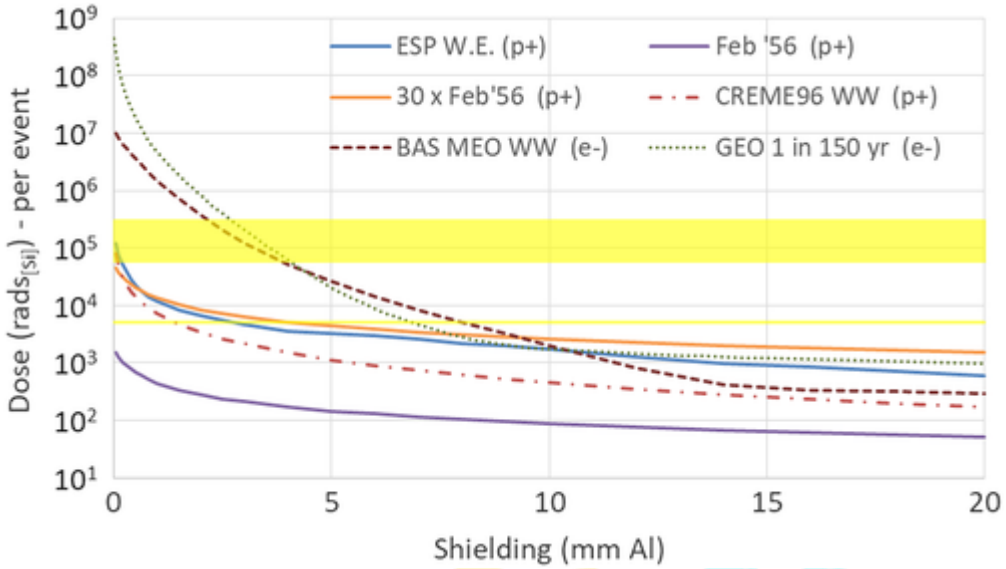

Figure 6

Dose-depth curves for four solar energetic particle event scenarios are compared to equivalent curves for two electron enhancement scenarios. "WW" refers to the *worst week* according to the CREME96 proton specification and medium Earth orbit (MEO) electron environment. Each curve is based on spherical shielding geometry with proton- and electron-based events labeled (p+) and (e−), respectively. The yellow line and band represent the 5 $krad_{[Si]}$ commercial off-the-shelf threshold and 50–300 $krad_{[Si]}$ tolerance range for rad hard components, respectively.

The different shape of proton dose-depth curves compared to electron dose-depth curves is apparent in this comparison. Protons penetrate further into shielding layers and, unlike energetic electrons, do not produce significant amounts of Bremsstrahlung radiation. The result is that the extreme electron enhancement scenarios yield many times the levels of proton event dose, even up to relatively high shielding depths of ~6 mm (with spherical geometry). At even higher shielding depths the most extreme SEPE scenarios become more significant, but only the IEC 1 in 1,000-year scenario (30 × Feb-56) exceeds the worst-case for electrons at GEO (which is based on a much shorter timescale), and only for shielding depths greater than 8 mm. Indeed, the similarity between worst-case GEO electron enhancement and the severe proton scenarios is striking at high shielding depths. At 10-mm shielding the ESP event dose of 1.76 $krad_{[Si]}$ slightly exceeds the GEO scenario dose of 1.73 $krad_{[Si]}$, although this is an isolated exception from the rule that the dose from our extreme electron scenario at GEO exceeds that from the worst-case event in the ESP model.

A more like-for-like comparison in terms of timescale is that between the CREME96 worst-week dose (based on a series of events nearly 30 years ago) and the worst-week at MEO according to the BAS model. The ratio between these two dose-depth curves is plotted in Figure 7. This ratio peaks at ~250 at 0.5 mm of Al shielding where the electron enhancement and solar proton dose values are 3.6 $Mrad_{[Si]}$ and 13.9 $krad_{[Si]}$, respectively. There is then a steady decline as direct ionizing dose from electrons reduces due to their attenuation, before a minimum ratio of ~1.5 is reached at around 15 mm of shielding. At this point the combined dose from both types of extreme event would be less than 1 $krad_{[Si]}$, thus potentially of little consequence in terms of damage to satellite components (although as an *additional* dose even this could push components beyond tolerance limits). The canonical 5 $krad_{[Si]}$ threshold for commercial off-the-shelf components is exceed by the MEO worst-case electron environment up to a spherical shielding level of 8 mm. The alternative slab shielding assumption would reduce calculated TID levels, due to the longer paths through shielding at shallow angles of incidence. However, this geometry is more applicable to the low levels of shielding for components close to the spacecraft surface and thus does not affect the high TID levels in well-shielded areas, which are of concern.

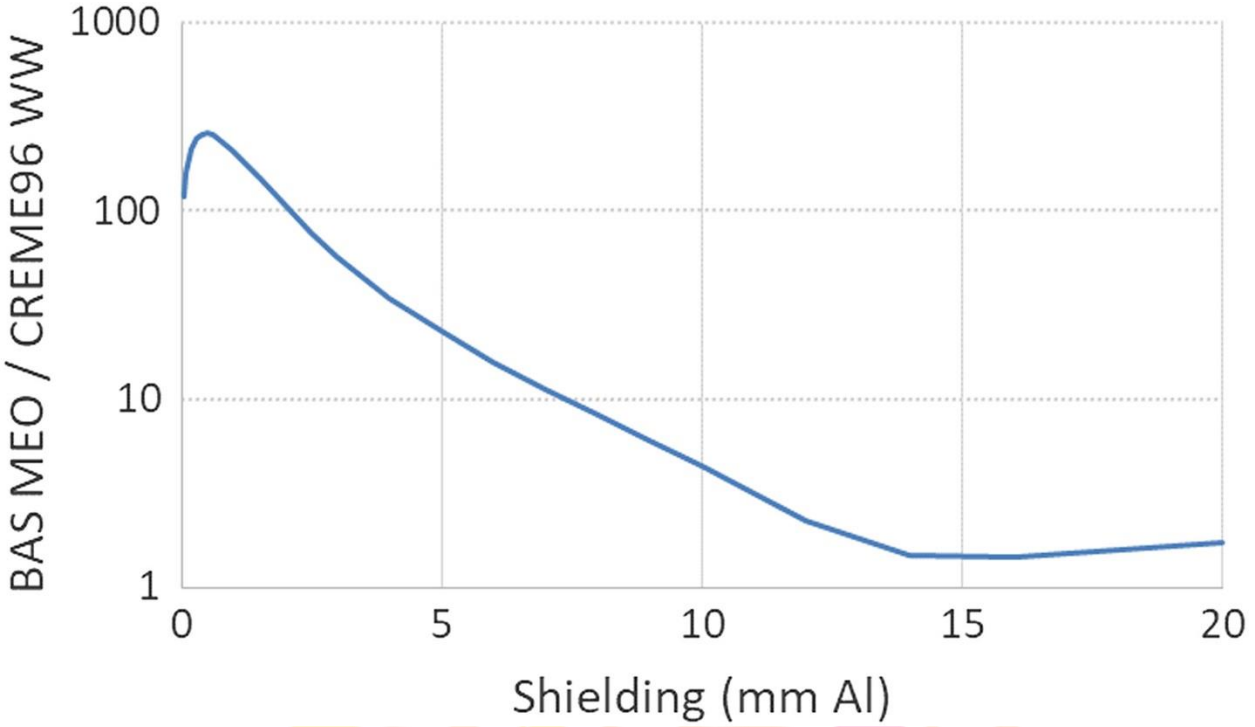

Figure 7
Dose ratio between the worst-week electron fluence in medium Earth orbit (MEO) and the worst-week proton fluence in CREME96. These two scenarios are chosen because the extrema are relevant to approximately the same timescale (~30 years). At all shielding depths the electron-induced dose exceeds the proton-induced dose.

From this comparison we conclude that the contribution to total dose from an extreme SEPE is likely to be small at MEO and GEO when compared to extreme electron enhancements. Magnetospheric shielding of solar protons would only accentuate this difference, especially if the SEPE were to occur during the equatorial passage of a MEO satellite, for example. It is possible that well-shielded parts of a spacecraft could experience significant additional dose (by fraction) from an extreme SEPE, but as the total dose would remain relatively low this is unlikely to result in substantial performance degradation. Hence, it is reasonable to conclude that the primary TID threat to GEO and MEO satellites from extreme space weather events is from trapped electrons rather than solar protons.

4 DDD

Displacement damage of atomic lattices can affect various components and systems on a spacecraft, especially those based on minority-carrier semiconductors such as bipolar junction transistors. However, the most conspicuous effect from a spacecraft survivability perspective is a loss of maximum power output (P_{max}) due to degradation of solar cells (Messenger et al., 2001). We use this as our metric to compare and contrast the engineering consequences of the enhanced environments under examination. Energetic electrons and protons both cause damage to solar cells by reducing minority carrier lifetimes within semiconductor layers. This damage occurs not as the result of ionization but to non-ionizing energy loss where atoms in the silicon lattice are displaced by incident radiation. Different approaches can be taken to try to quantify this effect in the space environment. A common method is to weight particle spectra by an energy-dependent relative damage coefficient (RDC) for each particle species, and then sum over all energies and particle species to produce a single value of equivalent fluence for incident 1-MeV electrons. RDCs are determined experimentally from the irradiation of solar cells with electrons and protons over wide energy ranges. As different particle species at different energies are attenuated to different degrees by solar cell coverglass shielding, this equivalent fluence parameter varies as a function of coverglass thickness. For GEO and MEO we compare the degradation of solar cells from extreme electron enhancements to the worst-case event in the ESP SEPE model. We do not include the Feb'56 event in this comparison, as the spectrum derived for this event is based on ground level data, and thus cannot be reliably extrapolated to the lower energies necessary for displacement damage calculation. As for the TID analysis, we use a 1 in 150-year event to represent the worst-case for the GEO electron environment (fluence calculated for one week duration) and for MEO we used the worst-week BAS model spectrum. For each of

these environments we calculate 1-MeV electron equivalent fluences as a function of coverglass thickness using the EQFLUX tool, accessible via the SPENVIS online system (www.spenvis.oma.be). We use the default input parameters for a single-junction gallium arsenide (GaAs) cell for all EQFLUX calculations. Results are plotted in Figure 8.

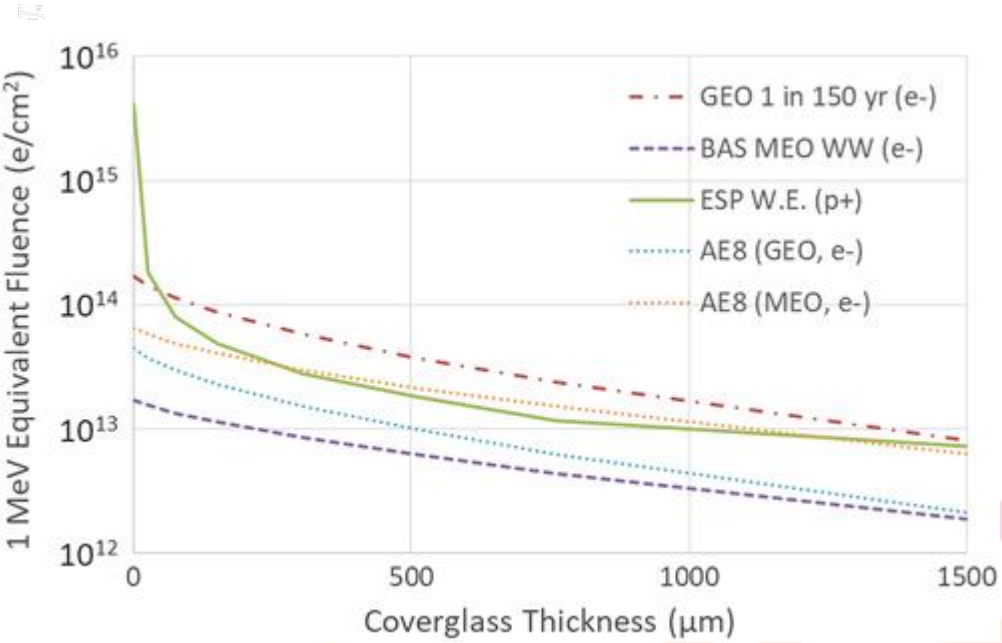

Figure 8

Equivalent 1 MeV electron fluences for two enhanced electron environments and the worst-case event in the emission of solar proton (ESP) proton fluence model, compared against annual equivalent fluences in medium Earth orbit (MEO) and geostationary Earth orbit (GEO). Fluences are plotted as a function of fused silica (2.2 g/cm^3) coverglass thickness for solar cells and are based on single junction gallium arsenide solar cells.

Two observations stand out from this comparison. First, for most coverglass thicknesses the 1 in 150-year storm at GEO, which is based on an AE8 spectral shape, leads to equivalent fluences that are significantly higher than either the extreme solar proton event or the worst-week at MEO from 30 years of data. At first glance this appears to be inconsistent with the dose comparison in Figure 6; however, that comparison was over a much wider range of shielding attenuation. The maximum coverglass thickness in our comparison is only 1,500 µm (1.5 mm); thus, lower energy particles play a much more dominant role, much like the greater dose at low shielding for the softer spectrum of the GEO environment. It is worth noting that the MEO environment would be far more severe if the orbit was equatorial rather than inclined to represent Galileo. The second observation is that the damage from the extreme proton event is closer to that from the extreme electron environments than is apparent for TID at low shielding levels. This is because the RDCs for protons increase substantially at lower energies, due to a greater transfer of elastic scattering energy to the recoil nucleus (Summers et al., 1993). In fact, below a coverglass thickness of approximately 50 µm, the equivalent fluence from a worst-case SEPE is dominant.

In order to understand these calculations in the context of damage to the power generating capability of solar cells, it is necessary to establish a relationship between displacement damage and power output. Such damage curves are determined empirically for different types of solar cells, with distinct degradation functions for protons and electrons. We use the MC-SCREAM tool (also available on SPENVIS) to calculate relative degradation of maximum power output (P_{max}) as a function of DDD (Messenger et al., 2001). We again consider both protons and electrons in our calculations. Figure 9 shows relative P_{max} degradation for annual GEO background, 1 in 150-year electron enhancement and ESP worst proton event, assuming a coverglass thickness of 100 µm. Damage curves showing the functional relationship between P_{max} and DDD are overlaid. Damage caused by protons and electrons is not identical when calculated as a function of DDD, as protons cause greater degradation for a given dose. For all MC-SCREAM calculations we use default parameters for a single-junction GaAs cell with a 100-µm coverglass of density 2.2 g/cm^3 and 10-µm semiconductor layer thickness.

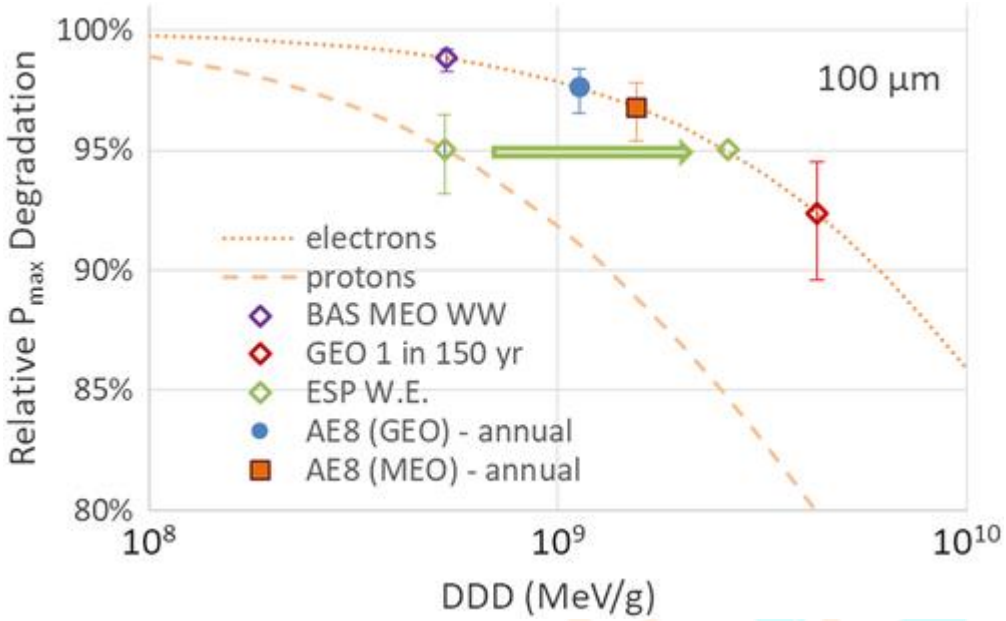

Figure 9
Power degradation versus displacement damage dose (DDD) curves is shown for electrons and protons for a single junction gallium arsenide solar cell. The emission of solar proton (ESP) model proton event results in a predicted 5% loss in power, whereas the figures for medium Earth orbit (MEO) worst-week and geostationary Earth orbit (GEO) 1 in 150-year electron environments are 1.2 and 7.6%, respectively. Annual degradation, based on the AE8 model, is also shown for both GEO and MEO. The error bars represent the impact on percentage degradation of a factor 1.5 change in DDD. The green arrow (and accompanying second green diamond) shows the equivalent position on the electron degradation curve of the ESP proton event.

Annual DDD in GEO (based on AE8) for this type of solar cell is predicted by MC-SCREAM to be 1.1×10^9 MeV/g, leading to an annual loss in power of 2.4% (for a Galileo orbit the annual degradation is 3.2%). The 1 in 150-year electron enhancement at GEO, adapted for one-week duration, results in approximately 4 times as much dose and 7.6% power reduction. By contrast the DDD from the ESP worst proton event is only 5.3×10^8 MeV/g, but based on the proton damage curve this corresponds to a loss of power of 5%, that is, equivalent to ~2 years of background degradation at GEO or ~1.5 years at MEO. The worst-week at MEO from the BAS 30-year reconstructed data set gives a significantly lower loss of power of only 1.2%, due to the combination of fewer low energy electrons and a shallow damage curve at low dose. As the damage curves are nonlinear (they follow a lognormal shape), the power loss caused by a given amount of displacement damage is somewhat dependent on timing—that is, how much power loss has already occurred in the lifetime of the spacecraft. The figures we have calculated are for extreme events occurring at the beginning of life, which is the worst-case in terms of solar cell degradation. We have also calculated equivalent figures for worst-case events occurring after one year of life. An ESP worst proton event occurring at this point would be expected to cause a 3.8% reduction in power generating capacity, rather than the 5% expected at the beginning of life. A 1 in 150-year electron enhancement at GEO after 1 year of operation would cause a 6.8% reduction in power, rather than 7.6% at the beginning of life. So although the timing of occurrence is a factor, such extreme events continue to pose a significant threat to power generation throughout the lifetime of a spacecraft.

This comparison reaffirms the conclusion of the TID analysis, namely, that an extreme electron enhancement can be more damaging than an extreme proton event, at least for this common type of solar cell. This is, of course, strongly dependent on the duration of the electron enhancement. If the electron enhancement were only sustained for two days, then the proton event could be more damaging (the comparison is also dependent to some extent on the power capacity *before* the onset of the events). In all cases the loss in power during an extreme event is only of the order of a few per cent. Hence, it is unlikely based on these assumptions that a major space weather event will cause widespread catastrophic failure of satellite operations due to solar cell damage. This analysis should not encourage complacency in the evaluation of solar cell damage in the event of extreme solar storms. For a given mission it would be prudent

to perform a similar analysis with bespoke parameters for the appropriate solar cell type and coverglass arrangement used on the spacecraft. However, we have shown that given that even a relatively quiescent outer electron belt already represents a hostile environment to solar cells and the additional damage caused by a very rare solar storm would probably have a manageable rather than a catastrophic effect.

5 Discussion

In this work the results of modeling and extreme value analyses are used to calculate the engineering consequences of extreme enhancements to the electron intensity in the Van Allen belts. The additional consideration of solar protons in order to evaluate the overall risks to spacecraft in MEO and GEO and what mitigation measures might be required are included.

The analysis indicates that the inclusion of solar protons has a relatively modest effect on worst-case scenarios for damage to spacecraft from both ionizing dose and solar cell degradation. The predicted dose from an extreme SEPE is eclipsed by both an extreme electron storm and the annual quiescent background (electron-induced) dose for aluminium shielding depths up to approximately 8 mm. At higher levels of shielding doses are significantly reduced. Therefore, even though the dose contribution from an extreme SEPE would be more significant by fraction, it would nevertheless be unlikely to cause widespread problems for spacecraft components. For solar cell degradation, the DDD from an extreme SEPE is less than that accrued due to trapped electrons during one year in the quiescent background at MEO or GEO. However, a steeper proton damage curve means that the degradation in maximum power output exceeds these annual background rates, based on a worst-case assumption of no geomagnetic attenuation. The impact of an extreme electron storm lasting approximately one week is greater still. Evidence from both theory and observation implies that this duration is highly plausible; therefore, the extreme electron enhancements are likely to be more of a threat to solar cell power capacity degradation than extreme solar energetic proton events. Hence, it seems that previous analyses (e.g., Odenwald et al., 2006; Odenwald & Green, 2007) of the implications of extreme events, which assumed that proton-induced solar damage was dominant, should be revisited.

For both the cumulative effects of ionizing dose and DDD, the consequence of an extreme (electron) storm can be thought of being equivalent to the rapid accumulation of up to four years' worth of ambient background exposure (perhaps more if sustained for more than a week). Therefore, the effect of such an event is to shorten the operational lifespan of the spacecraft by that same margin. For short lifetime missions, this implies the probable failure of various radiation-sensitive systems and a significant loss in power-generating capacity. For long lifetime missions, especially those that involve a fleet of satellites, a more likely consequence is to increase the rate at which the spacecraft need to be replaced. Given the high cost and complexity of establishing and maintaining a large satellite constellation, this would likely result in temporary or even permanent reduction in service provision, for example in GNSS platforms. Odenwald et al. (2006) estimated that a solar superstorm could result in an additional 87 satellites requiring replacement due to loss in power generating capability, at a cost of ~$24 billion. This may now be a conservative figure for the financial impact of satellite power degradation due to space weather. In part this is because the total satellite fleet has increased substantially in the decade since that estimate but also because our results suggest that the vulnerability to solar cell power degradation is even more acute for trapped electron enhancements. Predicting the true cost of such events is extremely difficult. Nonetheless, it is clear that relatively benign mitigation measures, such as increasing protective shielding above what is required for the mission environment *excluding* an extreme storm, could be very cost-effective.

Additional radiation effects that are not considered in this paper are SEE in spacecraft electronics, surface charging of spacecraft due to low-energy plasma electrons, and internal charging of dielectric materials within a spacecraft (Bodeau, 2010). The severity of all effects is determined not just by the environment but by the susceptibility of materials or components to incident radiation. For SEE, this range in susceptibility is extremely large, even varying substantially between ostensibly very similar components that have undergone minor changes in their manufacture process. As a result, any proper risk assessment for SEE vulnerability must be bespoke to a particular spacecraft, including a comprehensive list of all critical components used. Similarly, the vulnerability to surface charging, which is caused by a different particle population to the trapped electrons in the Van Allen belts, depends on a multitude of factors associated with the plasma environment and the engineering design of the spacecraft (Garrett, 1981). Whether

these would be dominant over high-energy-electron-induced failures during a contemporary trapped electron enhancement is indeterminable for the general case.

6 Conclusion

The results from state-of-the-art analyses of extreme space weather environments to calculate radiation effects on spacecraft is used. This work highlights the threat posed due to the cumulative damage mechanisms of TID and DDD. The key findings of this study may be summarized as follows:

1. The primary *extreme space weather* threat to spacecraft in terms of cumulative damage effects comes from trapped electrons rather than from solar protons.
2. The worst-week trapped electron environment for a Galileo spacecraft may result in up 250 times the level of ionizing dose caused by an equivalent worst-week event for solar protons.
3. Contemporary solar panels in geostationary orbit may suffer up to a 7.6% loss in power generating capacity in a 1 in 150-year solar storm.

Given these results, the economic analysis of the effect of ESW on the global satellite fleet should be updated as previous estimates assumed that for solar cell damage at least, solar protons are the dominant cause of lifetime reduction.

For the effects considered, a common theme is the need for an improved understanding of the system response. Variations in the different extreme environment scenarios are a source of considerable uncertainty. However, at least as important, is the uncertainty over how a material or electronic component or solar cell will react to well-defined changes in that environment. Therefore, a key part of designing a system to survive an extreme storm is preflight ground testing of the various components that comprise the spacecraft. Incorporating such testing into the design process, and using realistic test environments to minimize uncertainty, is a key recommendation from this work. Correlation of actual in-orbit behavior with moderate space weather events by flying onboard monitors will also be beneficial to improving the accuracy of calculations.

.

References

- Bodeau, M. (2010). High energy electron climatology that supports deep charging risk assessment in GEO, 48th AIAA Aerospace Sciences Meeting Including the New Horizons Forum and Aerospace Exposition. **https://doi.org/10.2514/6.2010-1608**
- ECSS-E-ST-10-04C (2008). Space engineering: The space environment.
- Garrett, H. B. (1981). The charging of spacecraft surfaces. *Reviews of Geophysics and Space Physics*, **19**(4), 577–616.
- Ginet, G. P., Madden, D., Dichter, B. K., & Brautigam, D. H. (2007). Energetic proton maps for the South Atlantic Anomaly, 2007 IEEE Radiation Effects Data Workshop. **https://doi.org/10.1109/redw.2007.4342532**
- Glauert S. A., (2016) Report on the 30 year high-energy electron re-construction for MEO, SPACESTORM project. **https://www.spacestorm.eu/**
- Glauert, S. A., Horne, R. B., & Meredith, N. P. (2014). Three-dimensional electron radiation belt simulations using the BAS radiation belt model with new diffusion models for chorus, plasmaspheric hiss, and lightning-generated whistlers. *Journal of Geophysical Research: Space Physics*, **119**, 268–289. **https://doi.org/10.1002/2013JA019281**
- Hands, A., Ryden, K., Underwood, C., Rodgers, D., & Evans, H. (2015). A new model of outer belt electrons for dielectric internal charging (MOBE-DIC). *IEEE Transactions on Nuclear Science*, **62**(6), 2767–2775. **https://doi.org/10.1109/tns.2015.2475134**
- Heynderickx, D., Quaghebeur, B., Wera, J., Daly, E. J., & Evans, H. D. R. (2004). New radiation environment and effects models in the European Space Agencys Space Environment Information System (SPENVIS). *Space Weather*, **2**, S10S03. **https://doi.org/10.1029/2004SW000073**

- Horne, R. B., Glauert, S. A., Meredith, N. P., Boscher, D., Maget, V., Heynderickx, D., & Pitchford, D. (2013). Space weather impacts on satellites and forecasting the Earths electron radiation belts with SPACECAST. *Space Weather*, **11**, 169–186. **https://doi.org/10.1002/swe.20023**
- Horne, R. B., & Pitchford, D. (2015). Space weather concerns for all-electric propulsion satellites. *Space Weather*, **13**, 430–433. **https://doi.org/10.1002/2015SW001198**
- IEC-TS 62396–6 (2017). Process management for avionics- atmospheric radiation effects. Part 6: Extreme space weather and potential impact on the avionics environment and electronics, Technical Report.
- Johnston, W. R., O'Brien, T. P., Ginet, G. P., Huston, S. L., Guild, T. B., & Fennelly, J. A. (2014). AE9/AP9/SPM: New models for radiation belt and space plasma specification, Sensors and Systems for Space Applications VII. **https://doi.org/10.1117/12.2049836**
- Lohmeyer, W., Carlton, A., Wong, F., Bodeau, M., Kennedy, A., & Cahoy, K. (2015). Response of geostationary communications satellite solid-state power amplifiers to high-energy electron fluence. *Space Weather*, **13**, 298–315. **https://doi.org/10.1002/2014sw001147**
- Maurer, R. H., Fretz, K., Angert, M. P., Bort, D. L., Goldsten, J. O., Ottman, G., et al. (2017). Radiation induced single event effects on the Van Allen Probes spacecraft. *IEEE Transactions on Nuclear Science*, **1–1**(11), 2782–2793. **https://doi.org/10.1109/tns.2017.2754878**
- Mekhaldi, F., Muscheler, R., Adolphi, F., Aldahan, A., Beer, J., McConnell, J. R., et al. (2015). Multiradionuclide evidence for the solar origin of the cosmic-ray events of AD 774/5 and 993/4. *Nature Communications*, **6**(1), 8611. **https://doi.org/10.1038/ncomms9611**
- Meredith, N. P., Horne, R. B., Isles, J. D., & Rodriguez, J. V. (2015). Extreme relativistic electron fluxes at geosynchronous orbit: Analysis of GOESE> 2 MeV electrons. *Space Weather*, **13**, 170–184. **https://doi.org/10.1002/2014sw001143**
- Meredith, N. P., Horne, R. B., Isles, J. D., Ryden, K. A., Hands, A. D. P., & Heynderickx, D. (2016). Extreme internal charging currents in medium Earth orbit: Analysis of SURF plate currents on Giove-A. *Space Weather*, **14**, 578–591. **https://doi.org/10.1002/2016sw001404**
- Messenger, S. R., Summers, G. P., Burke, E. A., Walters, R. J., & Xapsos, M. A. (2001). Modeling solar cell degradation in space: A comparison of the NRL displacement damage dose and the JPL equivalent fluence approaches. *Progress in Photovoltaics: Research and Applications*, **9**(2), 103–121. **https://doi.org/10.1002/pip.357**
- Messenger, S. R., Wong, F., Hoang, B., Cress, C. D., Walters, R. J., Kluever, C. A., & Jones, G. (2014). Low-Thrust Geostationary Transfer Orbit (LT2GEO) radiation environment and associated solar array degradation modeling and ground testing. *IEEE Transactions on Nuclear Science*, **61**(6), 3348–3355. **https://doi.org/10.1109/tns.2014.2364894**
- Meyer, P., Parker, E. N., & Simpson, J. A. (1956). Solar cosmic rays of February, 1956 and their propagation through interplanetary space. *Physical Review*, **104**(3), 768–783. **https://doi.org/10.1103/physrev.104.768**
- Miyake, F., Nagaya, K., Masuda, K., & Nakamura, T. (2012). A signature of cosmic-ray increase in AD 774–775 from tree rings in Japan. *Nature*, **486**(7402), 240–242. **https://doi.org/10.1038/nature11123**
- Odenwald, S. F., & Green, J. L. (2007). Forecasting the impact of an 1859-caliber superstorm on geosynchronous Earth-orbiting satellites: Transponder resources. *Space Weather*, **5**, S06002. **https://doi.org/10.1029/2006SW000262**
- Odenwald, S. F., Green, J. L., & Taylor, W. W. L. (2006). Forecasting the impact of an 1859-calibre superstorm on satellite resources. *Advances in Space Research*, **38**(2), 280–297. **https://doi.org/10.1016/j.asr.2005.10.046**
- Oldham, T., & Mclean, F. (2003). Total ionizing dose effects in MOS oxides and devices. *IEEE Transactions on Nuclear Science*, **50**(3), 483–499. **https://doi.org/10.1109/tns.2003.812927**
- Petersen, E. (1997). Predictions and observations of SEU rates in space. *IEEE Transactions on Nuclear Science*, **44**(6), 2174–2187. **https://doi.org/10.1109/23.659033**
- Rodgers, D. J., Hunter, K. A., & Wrenn, G. L. (2003). The FLUMIC electron environment model. In *in Proc. 8th Spacecraft Charging Technology Conf*. Huntsville, AL.
- Ryden, K. A., Morris, P. A., Hands, A. D. P., Dyer, C. S., Fellows, M., Taylor, B., et al. (2008). Radiation monitoring in medium Earth orbit over the solar minimum period, Published in Proceedings of RADECS 2008, 10th–12th September 2008, Jyvaskyla, Finland.
- Shea, M., & Smart, D. (1994). Significant proton events of solar cycle 22 and a comparison with events of previous solar cycles. *Advances in Space Research*, **14**(10), 631–638. **https://doi.org/10.1016/0273-1177(94)90518-5**

- Shea, M., Smart, D., McCracken, K., Dreschhoff, G., & Spence, H. (2006). Solar proton events for 450 years: The Carrington event in perspective. *Advances in Space Research*, **38**(2), 232–238. **https://doi.org/10.1016/j.asr.2005.02.100**
- Summers, G., Burke, E., Shapiro, P., Messenger, S., & Walters, R. (1993). Damage correlations in semiconductors exposed to gamma, electron and proton radiations. *IEEE Transactions on Nuclear Science*, **40**(6), 1372–1379. **https://doi.org/10.1109/23.273529**
- Taylor, B., Underwood, C. I., Evans, H. D. R., Ryden, K., Rodgers, D., Daly, E. J., et al. (2007). Results from the Galileo Giove—A radiation monitors and comparison with existing radiation belt models. *IEEE Transactions on Nuclear Science*, **54**(4), 1076–1081. **https://doi.org/10.1109/tns.2007.892115**
- Tylka, A. J., & Dietrich, W. (2009). A new and comprehensive analysis of proton spectra in ground-level enhanced (GLE) solar particle events, Proceedings of the 31st International Cosmic Ray Conference (Łódź).
- Usoskin, I. G., & Kovaltsov, G. A. (2012). Occurrence of extreme solar particle events: Assessment from historical proxy data. *The Astrophysical Journal*, **757**(1), 92. **https://doi.org/10.1088/0004-637x/757/1/92**

- Vette, J. I. (1991). The AE-8 trapped electron model environment, NSSDC, Rep. 91-24.Wrenn, G. L., Rodgers, D. J., & Buehler, P. (2000). Modeling the outer belt enhancements of penetrating electrons. *Journal of Spacecraft and Rockets*, **37**(3), 408–415. **https://doi.org/10.2514/2.3575**Xapsos, M., Summers, G., Barth, J., Stassinopoulos, E., & Burke, E. (1999). Probability model for worst case solar proton event fluences. *IEEE Transactions on Nuclear Science*, **46**(6), 1481–1485. **https://doi.org/10.1109/23.819111**Xapsos, M., Summers, G., Barth, J., Stassinopoulos, E., & Burke, E. (2000). Probability model for cumulative solar proton event fluences. *IEEE Transactions on Nuclear Science*, **47**(3), 486–490. **https://doi.org/10.1109/23.856469**Xapsos, M., Summers, G., Shapiro, P., & Burke, E. (1996). New techniques for predicting solar proton fluences for radiation effects applications. *IEEE Transactions on Nuclear Science*, **43**(6), 2772–2777. **https://doi.org/10.1109/23.556865**Rositsa Miteva, Mohamed Nedal, Astrid Veronig, Werner Pötzi, Parameter Study of Geoeffective Active Regions, Atmosphere, 10.3390/atmos15080930, **15**, 8, (930), (2024).
- William E. Parker, Richard Linares, Satellite Drag Analysis During the May 2024 Gannon Geomagnetic Storm, Journal of Spacecraft and Rockets, 10.2514/1.A36164, **61**, 5, (1412-1416), (2024).
- Xinyi Wang, Qiyong Wen, Changbo Ma, Guan Wang, Hongwei Xia, Guangcheng Ma, A Novel Fault Diagnosis Method for Dual-Angle Measurement System, 2024 43rd Chinese Control Conference (CCC), 10.23919/CCC63176.2024.10661571, (4955-4960), (2024).
- Kole Lutz, Space Pollution metals contributing to Ozone Hole, South Atlantic Anomaly, and Radiation Belt, Aeronautics and Aerospace Open Access Journal, 10.15406/aaoaj.2024.08.00202, **8**, 3, (152-159), (2024).
- Ibrahim B Mansir, Paul C Okonkwo, Naeim Farouk, Techno-economic optimization of a photovoltaic-wind energy-based hydrogen production system: A case study of different cities of Saudi Arabia, Energy & Environment, 10.1177/0958305X241248373, (2024).
- Yuxin Zhao, Xiaoning Yang, Yenan Liu, Yuming Liu, Yanlin Xu, Construction of Space Environmental Warning Model for ESD Anomalies in High Orbit Spacecraft, 2024 10th International Symposium on System Security, Safety, and Reliability (ISSSR), 10.1109/ISSSR61934.2024.00023, (143-149), (2024).
- Xin An, Anton Artemyev, Vassilis Angelopoulos, Xiao-Jia Zhang, Didier Mourenas, Jacob Bortnik, Xiaofei Shi, Nonresonant Scattering of Energetic Electrons by Electromagnetic Ion Cyclotron Waves: Spacecraft Observations and Theoretical Framework, Journal of Geophysical Research: Space Physics, 10.1029/2023JA031863, **129**, 3, (2024).
- B.A. Ojapinwa, E.O. Oyeyemi, A.O. Akala, IMF Bx, By, and Bz dependence of energetic particle precipitation in the magnetosphere, Advances in Space Research, 10.1016/j.asr.2024.07.060, (2024).
- Marina Stepanova, Victor Pinto, Elizaveta Antonova, Regarding the relativistic electron dynamics in the outer radiation belt: a historical view, Reviews of Modern Plasma Physics, 10.1007/s41614-024-00165-4, **8**, 1, (2024).
- Shuyan Wang, Qiang Wang, 2D Materials for Space Use , Two-Dimensional Materials for Nonlinear Optics, 10.1002/9783527838288.ch12, (303-332), (2024).
- Adnane Osmane, Emilia Kilpua, Harriet George, Oliver Allanson, Milla Kalliokoski, Radial Transport in the Earth's Radiation Belts: Linear, Quasi-linear, and Higher-order Processes, The Astrophysical Journal Supplement Series, 10.3847/1538-4365/acff6a, **269**, 2, (44), (2023).
- Dereje Seifu, Qing Peng, Kit Sze, Jie Hou, Fei Gao, Yucheng Lan, Electromagnetic Radiation Effects on MgO-Based Magnetic Tunnel Junctions: A Review, Molecules, 10.3390/molecules28104151, **28**, 10, (4151), (2023).

- Oleksandr Lobunko, Oleksandr Iskra, Substantiation of the protection system's technical outline for the aerospace objects, Scientific journal of the Ternopil national technical university, 10.33108/visnyk_tntu2023.04.102, **112**, 4, (102-114), (2023).
- Gabriele Ciarpi, Marco Mestice, Daniele Rossi, Fabrizio Palla, Sergio Saponara, A 10 Gb/s Line Driver in 65 nm CMOS Technology for Radiation-Pervaded and High-Temperature Applications, IEEE Access, 10.1109/ACCESS.2023.3297515, **11**, (76941-76952), (2023).
- Gulnur Akhtanova, Yerassyl Yerlanuly, Hryhorii P. Parkhomenko, Mykhailo V. Solovan, Andrii I. Mostovyi, Aliya K. Nurmukhanbetova, Alexander V. Kireyev, Igor V. Danko, Pavel A. Oreshkin, Timur K. Zholdybayev, Daniyar M. Janseitov, Tlekkabul S. Ramazanov, Viktor V. Brus, Electron Irradiation-Induced Degradation of TiN Thin Films on Quartz and Sapphire Substrates, ACS Omega, 10.1021/acsomega.3c07053, **9**, 1, (925-933), (2023).
- Devon Beck, Jacob Bickus, Ethan Klein, Paul Miller, Salvatore Di Cecca, Ryan Benz, Andrea Barney, Robert Longton, Austin Coon, Melissa Smith, Bradley Duncan, Additive Manufacturing of Multimaterial Composites for Radiation Shielding and Thermal Management, ACS Applied Materials & Interfaces, 10.1021/acsami.2c22478, **15**, 29, (35400-35410), (2023).
- Romain Buchs, Marie-Valentine Florin, Emmanuelle David, Jean-Paul Kneib, Gaps review and improvement pathways in the assessment and management of collision risk in low Earth orbit, Journal of Space Safety Engineering, 10.1016/j.jsse.2023.07.003, **10**, 3, (374-383), (2023)
- Qicong Li, Haijun Lou, Linli Zhu, Strain effect on the performance of proton-irradiated GaN-based HEMT, Applied Physics A, 10.1007/s00339-023-06631-z, **129**, 5, (2023).
- Wellen Rukundo, Solar Proton Activity over the Solar Cycle 24 and Associated Space Radiation Doses, Magnetosphere and Solar Winds, Humans and Communication, 10.5772/intechopen.103832, (2022).
- Nat Gopalswamy, The Sun and Space Weather, Atmosphere, 10.3390/atmos13111781, **13**, 11, (1781), (2022).
- Lin Quan, Yenan Liu, Ling Li, Dongya Wang, Kunpeng Wang, Li Xue, Wentang Wu, Yuxiong Xue, Yang Liu, Liang Luo, Study on Matching Between Environmental Warning Information and Spacecraft Anomalies, Journal of Spacecraft and Rockets, 10.2514/1.A35173, **59**, 5, (1455-1462), (2022).
- Alexey S. Belov, Features of generation and propagation of the extremely low frequency waves excited in the ionosphere under the powerful HF radioemission influence, Physics of Wave Processes and Radio Systems, 10.18469/1810-3189.2021.24.4.53-62, **24**, 4, (53-62), (2022).
- Meng Sun, Liang Liu, Tao Zhang, A Model of Addressing Abnormal Users in IP/LEO Satellite Communication System Based on Geographical Information Subnet, IEEE Access, 10.1109/ACCESS.2021.3139073, **10**, (2532-2545), (2022).
- D. Mourenas, A. V. Artemyev, X.-J. Zhang, V. Angelopoulos, Extreme Energy Spectra of Relativistic Electron Flux in the Outer Radiation Belt, Journal of Geophysical Research: Space Physics, 10.1029/2022JA031038, **127**, 11, (2022).
- Changhao Han, Zhaoyi Hu, Yuansheng Tao, Engang Fu, Yandong He, Fenghe Yang, Jun Qin, Xingjun Wang, Proton radiation effects on high-speed silicon Mach-Zehnder modulators for space application, Science China Information Sciences, 10.1007/s11432-022-3556-0, **65**, 12, (2022).
- Antonio Urbina, Antonio Urbina, Production of PV Modules, Sustainable Solar Electricity, 10.1007/978-3-030-91771-5_4, (85-130), (2022).
- Qiang Li, Yu Jiang, Yan Zhang, Yu Gao, Xiaohong Guo, Ruifei Cui, Sichen Wang, Wenming Guo, Tiexin Lv, Lifeng Cai, Lei Zhang, Xiaoying Li, Haichen Lin, Optimal attitude control for solar array orientation, Open Astronomy, 10.1515/astro-2021-0009, **30**, 1, (73-82), (2021).
- Saed Asaly, Lee-Ad Gottlieb, Yuval Reuveni, Using Support Vector Machine (SVM) and Ionospheric Total Electron Content (TEC) Data for Solar Flare Predictions, IEEE Journal of Selected Topics in Applied Earth Observations and Remote Sensing, 10.1109/JSTARS.2020.3044470, **14**, (1469-1481), (2021).
- Job Nijhuis, Quy Don Tran, Nam Nghiep Tran, Toan Dinh, Hoang-Phuong Phan, Nam Trung Nguyen, Tung Tran, Dusan Losic, Volker Hessel, Toward on-board microchip synthesis of CdSe vs. PbSe nanocrystalline quantum dots as a spectral decoy for protecting space assets , Reaction Chemistry & Engineering, 10.1039/D0RE00327A, **6**, 3, (471-485), (2021).

- Richard B. Horne, Sarah A. Glauert, Peter Kirsch, Daniel Heynderickx, Suzy Bingham, Peter Thorn, Babara-Ann Curran, David Pitchford, Ewan Haggarty, David Wade, Ralf Keil, The Satellite Risk Prediction and Radiation Forecast System (SaRIF), Space Weather, 10.1029/2021SW002823, **19**, 12, (2021).
- S. A. Glauert, R. B. Horne, P. Kirsch, Evaluation of SaRIF High-Energy Electron Reconstructions and Forecasts, Space Weather, 10.1029/2021SW002822, **19**, 12, (2021).
- Mike Hapgood, Matthew J. Angling, Gemma Attrill, Mario Bisi, Paul S. Cannon, Clive Dyer, Jonathan P. Eastwood, Sean Elvidge, Mark Gibbs, Richard A. Harrison, Colin Hord, Richard B. Horne, David R. Jackson, Bryn Jones, Simon Machin, Cathryn N. Mitchell, John Preston, John Rees, Neil C. Rogers, Graham Routledge, Keith Ryden, Rick Tanner, Alan W. P. Thomson, James A. Wild, Mike Willis, Development of Space Weather Reasonable Worst-Case Scenarios for the UK National Risk Assessment, Space Weather, 10.1029/2020SW002593, **19**, 4, (2021).
- Leonardo H. Regoli, Mark B. Moldwin, Connor Raines, Tom A. Nordheim, Cameron A. Miller, Martin Carts, Sara A. Pozzi, Radiation tolerance of the PNI RM3100 magnetometer for a Europa lander mission, Geoscientific Instrumentation, Methods and Data Systems, 10.5194/gi-9-499-2020, **9**, 2, (499-507), (2020).
- Milla M. H. Kalliokoski, Emilia K. J. Kilpua, Adnane Osmane, Drew L. Turner, Allison N. Jaynes, Lucile Turc, Harriet George, Minna Palmroth, Outer radiation belt and inner magnetospheric response to sheath regions of coronal mass ejections: a statistical analysis, Annales Geophysicae, 10.5194/angeo-38-683-2020, **38**, 3, (683-701), (2020).
- A. D. P. Hands, H. Evans, K. A. Ryden, I. Sandberg, D. Heynderickx, G. Provatas, S. Aminalragia-Giamini, A. Tsigkanos, C. Papadimitriou, D. Rodgers, An Update to MOBE-DIC Using Current Monitor Measurements From Galileo, IEEE Transactions on Nuclear Science, 10.1109/TNS.2019.2944699, **67**, 1, (181-190), (2020).
- J.-F. Ripoll, S. G. Claudepierre, A. Y. Ukhorskiy, C. Colpitts, X. Li, J. F. Fennell, C. Crabtree, Particle Dynamics in the Earth's Radiation Belts: Review of Current Research and Open Questions, Journal of Geophysical Research: Space Physics, 10.1029/2019JA026735, **125**, 5, (2020).
- Alexander R. Lozinski, Richard B. Horne, Sarah A. Glauert, Giulio Del Zanna, Daniel Heynderickx, Hugh D. R. Evans, Solar Cell Degradation Due to Proton Belt Enhancements During Electric Orbit Raising to GEO, Space Weather, 10.1029/2019SW002213, **17**, 7, (1059-1072), (2019).
- Yihua Zheng, Natalia Yu Ganushkina, Pier Jiggens, Insoo Jun, Matthias Meier, Joseph I. Minow, T. Paul O'Brien, Dave Pitchford, Yuri Shprits, W. Kent Tobiska, Michael A. Xapsos, Timothy B. Guild, Joseph E. Mazur, Maria M. Kuznetsova, Space Radiation and Plasma Effects on Satellites and Aviation: Quantities and Metrics for Tracking Performance of Space Weather Environment Models, Space Weather, 10.1029/2018SW002042, **17**, 10, (1384-1403), (2019).
- S. A. Glauert, R. B. Horne, N. P. Meredith, A 30-Year Simulation of the Outer Electron Radiation Belt, Space Weather, 10.1029/2018SW001981, (2018).